

## Improved Precision in the Evaluation of Ion-Sensitive Photoplates by a Computer Program

J. FRANZEN and K. D. SCHUY

Max-Planck-Institut für Chemie (Otto-Hahn-Institut), Mainz

(Z. Naturforschg. 21 a, 1479—1488 [1966]; received 10 May 1966)

An algorithm is presented to be used in the computer evaluation of ion-sensitive photographic plates in spark source analyses by mass spectroscopy. It is shown that this algorithm permits the attainment of the precision of photoplate evaluation demanded by theory, i. e. a precision of 0.015 relative standard deviation of the measured ion density for a mass spectral line of area 0.05 mm<sup>2</sup>.

The photographic plate still represents the most useful tool for ion detection in the mass spectrographic analysis of solids with spark sources: the most striking advantage of the photoplate is its ability to concurrently integrate the hundreds of separated ion currents of the mass spectrum, regardless of their fluctuation with time. All elements contained in the sample are detected simultaneously, the information being stored by the emulsion. After extracting the information which is of immediate interest, the spectroscopist may, at any later date, refer to the spectra again should his interest be aroused in some other phenomenon.

However, the quantitative evaluation of the photoplate is a rather lengthy and tedious procedure. In contrast to ordinary practice in emission spectroscopy, even the most trivial evaluation of ion-sensitive emulsions necessitates the determination of a calibration curve, not only for different emulsion batches but for every plate separately. More precise methods require even more than one calibration curve per plate<sup>1</sup>. The calibration curve permits the conversion of measured line transparencies to ion densities. In all customary methods known to us, this conversion is done graphically, i.e. the measured transparency values are plotted on some suitable scale, and the transparency curve is fitted by eye to the measured values. On one hand, the results obtained with these methods depend on the skill of the individual; on the other hand, they are subject to subconscious falsification of results due to a knowledge of previous analyses and tabulated

isotope abundance ratios. Depending on whether the analyst is ambitious or unconcerned, the results are either not as good as they could be, or they are better than theory permits. Furthermore, by manual evaluation it is next to impossible to obtain and consider such information as, e.g., the variation of saturation transparency, or the variation of the slope of the transparency curve, with ion mass and energy. The complexity of the problem as well as the large quantity of available data calls for a computer program for the efficient treatment of the task.

To our knowledge, there have been two computer programs described in the literature so far. KENNICOTT's program<sup>2</sup> makes use of the long-known CHURCHILL two-line method<sup>3</sup>. This method, while perhaps being quite useful in emission spectroscopy, has serious drawbacks when used in the evaluation of ion-exposed plates. As used by KENNICOTT, it requires the line transparencies of just two isotopes of one element which must have an abundance ratio between 1.2 and 3. Many analysts rejoice when they obtain smooth transparency curves of elegant appearance. However, the neat appearance of the curves must not mislead the analyst to believe them to be correct. Even small errors associated with the ion density ratio of the two lines employed will be raised to the 10th to 20th power, depending on the number of steps performed during the construction of the curve. This might lead to extremely flat or to extremely steep curves. An error in the ion density ratio might be caused by a variety of effects: the

<sup>1</sup> In the following, the terms "calibration curve" and "transparency curve" are used synonymously: a transparency curve for an element of given charge is, in fact, always the calibration curve of the emulsion for this ion species.

<sup>2</sup> PH. R. KENNICOTT, 12th Ann. Conf. Mass Spectrometry and Allied Topics, paper no. 93, Montreal, P.Q., Canada, 1964.

<sup>3</sup> J. R. CHURCHILL, Ind. Eng. Chem., Anal. Edition 16, 653 [1944].



majority of tabulated isotope abundance ratios is uncertain by 0.5 to 1% or more<sup>4</sup>; isotope discrimination might occur in the ion source; the variation of photographic sensitivity with isotope mass has not yet been investigated and may not coincide with the variation of photographic sensitivity with ion mass for different elements<sup>5</sup>; photographic sensitivity or background might vary along the photoplate. As an example, Fig. 1 shows two transparency curves

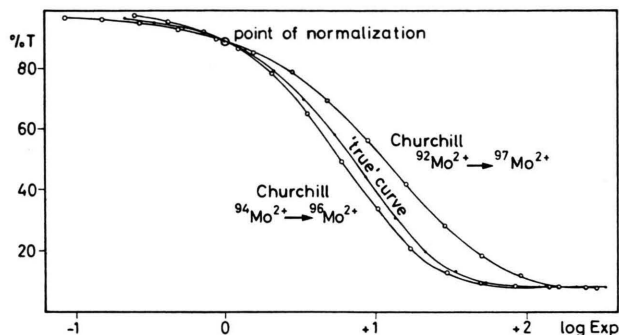


Fig. 1. The plot demonstrates the unreliability of the CHURCHILL two-line method in mass spectroscopic work. Both CHURCHILL calibration curves were most carefully constructed, but they differ from each other by a factor of 2.4 at 20%  $T$ . The "true" curve is a least-square fit of all experimental points to eq. (1), using the abundance ratios of all isotopes, and all exposure ratios.

obtained from two different molybdenum isotope pairs on the same plate. The transparency curve is systematically too flat if the lower mass is more abundant than the higher mass, and too steep otherwise. Normalizing the two curves at a transparency  $T = 90\%$ , we note that the ion densities obtained at  $T = 20\%$  differ from each other by a factor of 2.4, i.e. it is impossible to produce any precise analyses. Last but not least, we consider it absurd to discard all information available on other isotope abundances as well as the exposure ratios indicated by the monitor, and to resort to just one ratio and

its accidental uncertainty. Maximum information should be employed for the construction of the calibration curve, as it constitutes the basis of all future evaluation of the plate.

WOOLSTON<sup>7</sup> has based his computer program on an empirical equation for the transparency curve suggested by HULL<sup>8</sup>. Although, because of its empirical character and its limited validity, the HULL formula is open to some criticism<sup>9</sup>, it is nevertheless much to be preferred to the CHURCHILL two-line method. In principle it is feasible to use a large quantity of data (all isotopes and all exposures of a chosen element of given charge) for the construction of the calibration curve by optimizing both the slope parameter  $R$  and the saturation transparency  $T_s$ . Unfortunately, WOOLSTON decided to use only three data points (spectral lines) for a given component because he wished to have just one punch card for each component. Although he sets up a transparency curve for each component, we believe that just three points with their accidental deviations are insufficient to reliably fix the calibration curve. We feel that the intrinsic precision of the photoplate cannot be fully exposed to view by this method.

With the above considerations in mind, we have developed a computer program which is based on the theoretical equation of the transparency curve reported recently<sup>9</sup>. This program, which has run since the spring of 1965, allows the full utilization of the intrinsic photoplate precision which is determined by the statistics of developed grains.

### Scope of the Program

The program takes over just one part of the total analysis procedure: the processing of the transparency values of such lines which have previously been identified visually, and photometered<sup>10</sup>.

<sup>4</sup> P. J. DE BIÈVRE, M. G. GALLET et G. H. DEBUS, The Atomic Weights as Computed from Nuclidic Masses and Isotope Abundances, 3rd preliminary report, Central Bureau for Nuclear Measurements, EURATOM/Geel (Belgium), July 1965.

<sup>5</sup> KREBS<sup>6</sup> has shown this non-coincident behaviour of isotope mass sensitivity and ion mass sensitivity for different elements in case of an ion-detecting secondary-electron multiplier.

<sup>6</sup> K. KREBS, Humboldt University, Berlin, private communication.

<sup>7</sup> J. R. WOOLSTON, 14th Ann. Conf. Mass Spectrometry and Allied Topics, paper no. 17, St. Louis, Miss., 1965.

<sup>8</sup> C. W. HULL, 10th Ann. Conf. Mass Spectrometry and Allied Topics, paper no. 72, New Orleans, La., 1962.

<sup>9</sup> J. FRANZEN, K. H. MAURER, and K. D. SCHUY, Z. Naturforsch. **21a**, 37 [1966].

<sup>10</sup> Up to now, the complete automation of line identification and photometer transparency measurements would not be justified financially; nor would it save any time, as these steps are easy to learn, and quickly reduce to a routine matter for the analyst. However, a manually operated photometer with digitized data output on paper or magnetic tape is much to be desired.

In order to make the program capable of adequately coping with the different tasks arising in spark source mass spectroscopy, we have decided on the outset to make it as flexible as possible. In fact, we required it to perform the following modes of operation:

*Modus 1:* Elemental analysis relative to 1–3 internal reference elements, without correction of elemental sensitivity factors.

*Modus 2:* Elemental analysis corrected for sensitivity factors obtained previously from reference samples. The sensitivity factors are part of the input data.

*Modus 3:* Calculation of elemental sensitivity factors of the ion source, using the known elemental concentrations of reference samples.

*Modus 4:* Determination of characteristic values of the emulsion calibration curve. This *modus* permits the investigation of, say, the variation of the absolute photographic sensitivity along a plate, or the variation of the calibration curve parameters for ions of different mass, charge, and energy.

*Modus 5:* Computation of the abundance ratios of molecular ions (ion clusters).

*Modus 6:* Computation of isotope abundance ratios, automatically referred to sum of all ions = 100%, most abundant isotope = 100%, and least abundant isotope = 1.

*Modus 7:* Computation of isotope abundance ratios using a reference mass spectrum on the same plate. This mode of operation eliminates the variation of the photographic sensitivity along the plate, and any possible mass discrimination in the source.

*Modus 8:* Calculation of elemental concentrations using a mass spectrum of a reference sample on the same plate. In addition to correcting the analysis for elemental sensitivity factors, this mode also corrects for the variation of photographic sensitivity and mass discrimination, as done in *modus 7*. *Modus 8* yields the most precise analyses and should be used whenever possible.

*Modus 9:* Elemental analysis by comparison of an unknown spectrum with a reference spectrum on a different plate. This *modus* shortcuts *modi 2* and *3* in such cases where the output of elemental sensitivity factors is of no interest.

Furthermore, there are a number of input marks which control details of the program:

*Line width:* In case there is no regular increase of line width with mass according to some law (e.g. a  $\sqrt{m}$ -increase for the MATTAUCH-HERZOG geometry), measured line widths can be used for correction.

*Mass and energy dependence of the photographic sensitivity:* Any one of the relationships known in the literature so far may be chosen.

*Units:* The figures of the analyses may be printed out in %, ppm, parts atomic or by weight.

Further input numbers control whether background correction is made or not, whether the transparency curve is printed out, whether individual analyses for each isotope of an element are desired, whether one wants all isotopes analysed together, or whether a transparency curve is to be computed from any new set of input data.

### Mathematical Basis

The computer program is chiefly based on theoretically derived equations<sup>9</sup> which, up to this date, appear to give best agreement with experimental values. The equations were derived particularly with their application to a computer program in mind.

#### a) Transparency curve:

$$T_1 = T_s + \frac{1 - T_s}{[1 + e N/V(1 - T_s)]^V} \quad (1)$$

$T_1$  = line transparency,  $T_s$  = saturation transparency (transparency for large exposures, but still within the range of primary blackening),  $e = [d(1 - T)/dN]_{N \rightarrow 0}$  = photographic sensitivity,  $N$  = number of ions incident per unit area,  $V$  = parameter of the size-frequency distribution of the AgBr grain impact areas.  $V$  governs the slope of the transparency curve.

#### b) Correction of transparency $T$ for ion-produced background fog:

$$T_1 = 1 - \frac{(T_b - T_{1+b})(1 - T_s)}{T_b - T_s}; \quad (2)$$

$T_1$  = line transparency corrected for background fog,  $T_b$  = transparency of background fog,  $T_{1+b}$  = transparency of line plus (superimposed) background as measured with the photometer.

This equation is rigorously valid only for background fog produced by ions having the same penetration depth into the emulsion as those which have produced the line, but also holds to good approxi-

mation in case of fog produced by other ions of the spectrum. For fog due to light quanta or plate storage, this equation is invalid. However, in practice this type of fog is in general small and evenly distributed across the plate so that corrections by Eq. (2) cancel out.

c) *Sensitivity loss of the photoplate due to background fog:*

$$\varepsilon = [(T_b - T_s)/(1 - T_s)]^{1/V}. \quad (3)$$

$\varepsilon = e_{\text{corr}}/e_{\text{uncorr}}$  = factor of the sensitivity loss,  $e_{\text{corr}}$ ,  $e_{\text{uncorr}}$  = photographic sensitivity after and before correction.

The range of validity of eq. (3) is smaller still than that of eq. (2). It critically depends on the ion penetration depth and must therefore be used with caution. In general, however, eq. (3) considerably improves the analytical results. The effect of the corrections by eqs. (2) and (3) is the same as the method described by some authors<sup>8, 11</sup> to subtract an apparent ion density of the background fog as obtained from the transparency curve, from the ion density of line plus background. Eqs. (2) and (3) have the advantage of exposing the physics involved, and enable the separation of the influence of background fog on line transparency and emulsion sensitivity.

d) *Ion density and elemental concentration:*

In addition to eqs. (1) to (3) we need a relation connecting the ion density  $N$  producing a given line with the concentration  $C(\text{element})$  of the respective element in the sample:

$$N = \frac{C \cdot s \cdot Q \cdot h}{b \cdot l} \quad (4)$$

where

$C(\text{element})$  = element concentration in the sample,

$s(\text{element, charge})$  = relative sensitivity of the ion formation and extraction process for a given element and charge, referred to the sum of all ions in the beam arriving at the monitor detector,

$Q$  = exposure of the photoplate as measured by the monitor detector,

$h(\text{isotope})$  = isotope abundance,

$b(\text{mass/charge})$  = effective line breadth,

$l(\text{mass/charge})$  = effective line length. This length is equal to the line length that would appear were

there no limiting apertures in the beam. The effective line length should not be set equal to the line length visible on the photoplate. For mass spectrographs without z-focussing, the effective line length is proportional to the length of the ion trajectory from the focal point of the ion source to the point of incidence on the photographic plate.

e) *Photographic sensitivity:*

The photographic sensitivity  $e$  is given by

$$e = e_{\text{abs}} \cdot e_{\text{rel}} \cdot \varepsilon, \quad (5)$$

where

$e_{\text{abs}}(\text{plate})$  = absolute sensitivity of the photographic plate for ions of mass 1 and energy 1,

$e_{\text{rel}}(\text{mass, energy})$  = sensitivity of photographic plate for ions of given mass and energy relative to ions of unit mass and energy,

$\varepsilon(\text{fog})$  = factor of sensitivity loss of the photographic plate due to background fog [viz. eq. (3)].

With these five equations, all tasks required by modus 1 to modus 9 can be tackled. In order to economize the program, the algorithm should be set up such that it can be used by the machine with little alterations for all tasks.

The transparency curve eq. (1) contains the quantity  $e \cdot N$  which, with the aid of eqs. (4) and (5), can be written

$$e \cdot N = q_1 \cdot P_1. \quad (6)$$

The factor

$$q_1 = \frac{e_{\text{rel}} \cdot \varepsilon \cdot h \cdot Q}{b \cdot l} \quad (7)$$

contains all *known* quantities of eqs. (4) and (5).  $q_1$  may be thought of as a "normalized exposure": all lines of one element and one charge which have been exposed with the same  $q_1$ , exhibit the same background-corrected transparency  $T_1$  regardless of their mass, isotope abundance, line area, or background fog. All number pairs  $(q_1, T_1)$  of the lines of one element and one charge lie on a smooth curve (the transparency curve) when plotted as  $T_1$  vs  $q_1$  or as  $T_1$  vs  $\log q_1$ . This curve is represented with high accuracy by eq. (1).

The experimental values  $T_{1+b}$ ,  $T_b$ , and  $Q$  measured for each line are — immediately after having been read — converted to  $T_1$  and  $q_1$  according to eqs. (2) and (7). The values  $T_{1+b}$ ,  $T_b$ , and  $Q$  are then no longer required for the computation and, therefore, need not to be stored. It should be noted that the direct conversion of the measured

<sup>11</sup> E. B. OWENS and N. A. GIARDINO, Anal. Chem. **35**, 1172 [1963].



value triple ( $T_{1+b}$ ,  $T_b$ ,  $Q$ ) into the pair ( $T_1$ ,  $q_1$ ) has become feasible because the total background correction has been split up into a correction for transparency [eq. (2)], and a sensitivity loss factor [eq. (3)] which corrects for the exposure.

The second factor of eq. (6),

$$P_1 = C \cdot e_{\text{abs}} \cdot s \quad (8)$$

combines the three *unknown* quantities (elemental concentration, absolute photographic sensitivity, and relative sensitivity of ion formation). These  $P_1$ -values are of paramount importance for the future progress of the program: all tasks required by modus 1 to modus 9 reduce to a determination of one of the factors contained in eq. (8). Modus 3 asks for the relative sensitivity  $s$  of ion formation, in modus 4 the absolute photographic sensitivity  $e_{\text{abs}}$  of the plate is wanted, and the remaining modi require the concentration  $C$  in the sample to be found. Therefore, the different modi are distinguished just by the means with which the respective unknown quantities of eq. (8) are eliminated.

Provided the transparency curve for the given element and for the given charge is known, i.e. the slope  $V$  and the saturation transparency  $T_s$  have already been computed, then the  $P_1$ -value for each line can be found from the pair ( $T_1$ ,  $q_1$ ) by

$$P_1 = \frac{V \cdot (1 - T_s)}{q_1} \left[ \left( \frac{1 - T_s}{T_1 - T_s} - 1 \right)^{1/V} \right]. \quad (9)$$

Since all pairs ( $T_1$ ,  $q_1$ ) for all lines of one element and one charge should lie on the same transparency curve, they should all yield the same  $P_1$ -value. Because of transparency fluctuations due to grain statistics, and because of unavoidable experimental errors, the  $P_1$ -values obtained from different lines (different isotopes of one element, different exposures) will not be identical but will vary statistically. To obtain a single  $P_1$ -value for all lines of one element and one charge, the different  $P_1$ -values must be averaged. This procedure corresponds exactly to the manual method of plate evaluation described above: a "mean" transparency curve is drawn by eye through the totality of experimental points plotted as  $T$  vs log exposure.

Every worker in the field knows that reliable curve fitting by eye is the weakest part of manual plate evaluation. The computer cannot be bribed; it is not susceptible to subjective errors, and the averaging is done with utmost precision and reproducibility.

Upon inspection of a typical transparency curve (see Fig. 2), it is evident that not every  $P_1$ -value should be used with the same confidence: different weights have to be attached to them. From Fig. 2 we immediately learn that, for equal variations in

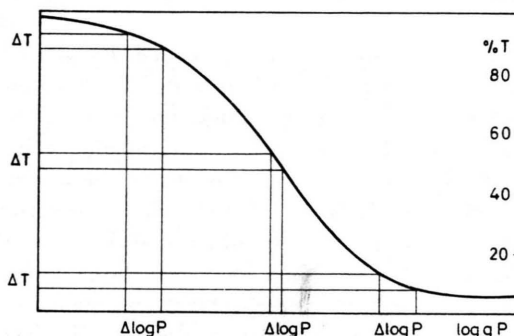


Fig. 2 demonstrates the weights of log  $P$  being proportional to the slope of the transparency curve  $T$  vs. log  $q P$ .

line transparency, the weights of  $P_1$  are proportional to the slope of the transparency curve  $T_1$  vs log ( $q_1 P_1$ ), i.e. the weights are proportional to

$$\left( \frac{dT}{d \log(q P)} \right)_1 = \left( \frac{T_1 - T_s}{1 - T_s} \right) - \left( \frac{T_1 - T_s}{1 - T_s} \right) \left( \frac{T_1 - T_s}{1 - T_s} \right)^{1/V}. \quad (10)$$

However, the statistical fluctuations of the measured transparency values are not constant but are, by and large, proportional to  $\sqrt{1 - T_1}$  (within the range of normal grain dispersion in the emulsion<sup>9</sup>). Therefore, we obtain the weights of  $P_1$  by

$$W_1 = \left( \frac{dT}{d \log(q P)} \right)_1 \cdot \sqrt{1 - T_1} \quad (11)$$

Furthermore, because it is empirically established that not the values  $P_1$  but their logarithms lie on a normal distribution, we average the  $P_1$ -values geometrically:

$$\bar{P} = \exp \frac{\sum W_1 \ln P_1}{\sum W_1}. \quad (12)$$

The corresponding standard deviation

$$\sigma(\ln \bar{P}) = \sqrt{\frac{\sum (\ln P_1 - \ln \bar{P})^2}{n - 1}}, \quad (13)$$

$n$  = number of lines measured, yields the standard deviation factor

$$F(\bar{P}) = \exp[\sigma(\ln \bar{P})] \quad (14)$$

of the individual  $P_1$ -values. For large deviations, the choice of a standard deviation factor  $F$  is much more reasonable than the standard deviation  $\sigma$ .

$F$  determines the deviation analogously to  $\sigma$ : about 68% of all  $P_1$ -values lie within the range  $\bar{P}/F$  and  $\bar{P} \cdot F$ , about 95% lie within  $\bar{P}/2F$  and  $\bar{P} \cdot 2F$ , and about 99.7% lie within  $\bar{P}/3F$  and  $\bar{P} \cdot 3F$ . For small deviations ( $F < 1.2$ ), the value  $F - 1$  is approximately equal to the relative standard deviation  $\sigma(P)/\bar{P}$  of the individual  $P_1$ 's.

If one or more of the calculated  $P_1$ -values lie outside the range of  $\bar{P}/XF$  and  $\bar{P} \cdot XF$ ,  $X$  being a prechosen factor, these values are automatically discarded by the computer, and printed out if so desired. This elimination process has been found extremely useful: areas of the gelatin containing no silver grains, or fine objects sticking to the emulsion surface, or other marks on the plate often make a transparency measurement erroneous much beyond the ordinary experimental error. The factor  $X$  depends on the abundance of such erroneous measurements. For ILFORD Q2 emulsions a value of  $X = 2.25$  was found satisfactory. If none of the eliminated lines were disturbed by emulsion flaws but would just show statistical fluctuations, then 97.56% of all  $P_1$ -values should lie within the range  $\bar{P}/2.25F$  and  $\bar{P} \cdot 2.25F$ . Therefore, the probability of "good" experimental values having been discarded is small.

### The Calibration Curve and its Determination

To keep the mathematics clear, we have assumed above that the calibration curve (which is determined by the quantities  $V$  and  $T_s$ ) is known. Before describing the method by which the calibration curve is found, some remarks concerning the character of  $V$  and  $T_s$  are in order. Neither  $V$  nor  $T_s$  are constant for different ion species. With decreasing ion mass and increasing ion energy, the slope parameter  $V$  of the transparency curve increases, the saturation transparency  $T_s$  decreases. The law governing this behaviour is linked with the depth of ion penetration into the emulsion but has not yet been investigated.

In most practical cases, the value  $T_s$  can be measured for a large number of lines. For intermediate ion species,  $T_s$  can then be interpolated to sufficient accuracy. The input data contain both measured and interpolated  $T_s$ -values. The parameter  $V$  presents some difficulties: it cannot be measured directly from the plate but must be found by the computer through an analysis of the shape of the

transparency curve  $T_1$  vs  $\log q_1$ . Since the dependence of the final analysis on the parameter  $V$  is not too critical, and since the determination of  $V$  is a rather time-consuming process even with a computer, we have in zeroth approximation decided to determine  $V$  just once for an analysis, and hold it constant. In the program, there is an as yet empty procedure provided which shall take care of the dependence of  $V$  on ion mass and energy and which shall be filled once the exact relationship is known. At present, for precise analyses, we divide the plate into several regions, determine  $V$  for the different regions, and perform separate analyses for each region. As an example, in the analysis of a stainless steel sample, we analyze  $\text{Cu}^+$ ,  $\text{Ni}^+$ ,  $\text{Co}^+$ ,  $\text{Fe}^+$ ,  $\text{Mn}^+$ ,  $\text{Cr}^+$ ,  $\text{V}^+$ , and  $\text{W}^{3+}$ ,  $\text{Sn}^{2+}$ ,  $\text{Mo}^{2+}$ , and  $\text{Nb}^{2+}$  with the same  $V$ -value, and use different  $V$ -values for the analysis of doubly- and triply-charged ions of the iron group. This method has yielded very satisfactory results in the past; we have found very nearly the same  $V$ -value to hold for one such group.

The computer determines the parameter  $V$  by fitting the experimental values to the theoretical curve, using the method of least squares. If there exists no exact solution of the equation for the minimum of the squared deviations, a successive approximation is performed by stepwise alteration of  $V$  and  $T_s$ . The optimizing process commences with the measured (or interpolated)  $T_s$ -value and a fixed  $V$ -value of suitable magnitude. First  $\bar{P}$  is computed from the  $T_1$ - and  $q_1$ -values of a chosen element of given charge.  $\bar{P}$  determines the position of the calibration curve within the  $T_1$  vs  $\log(p_1 P_1)$  coordinate system. Then the differences between the measured  $T_1$ -values and the corresponding  $T$ -values given by the theoretical curve are computed for each  $q_1$ . They are squared and summed over all experimental points, and the results stored. This process is repeated with a slightly altered  $T_s$ -value until the minimum of the sum of the squared deviations has been found. Then  $V$  is slightly changed, and the above process repeated. This continues until the absolute minimum with respect to  $V$  and  $T_s$  is found. The parameters of the calibration curve,  $V$  and  $T_s$ , may be printed out, together with the standard deviation of these values, the number of lines used, and the number of steps performed during the optimizing process. If desired, the pair  $(T_1, \log q_1)$  of each line as well as the

tabulated theoretical calibration curve may be printed out for inspection or demonstration. Again, all experimental values exceeding the standard deviation by a prechosen factor  $X$  may be eliminated during the computation, and printed out with the results. It should be noted that the entire optimizing process is repeated once an experimental point has been eliminated. Of course, the  $V$  and  $T_s$  found at the instant of elimination of an experimental value are used as new starting values.

### Program Operation

A simplified flow chart of the program is shown in Fig. 3. In step 1, the pertinent auxiliary data of the analysis are read: modus number; analysis number; number of plate and sample; information on the ion source, mass spectrograph, and emulsion; the reference elements desired (only for modus 1-3); the marks controlling the law of photo-

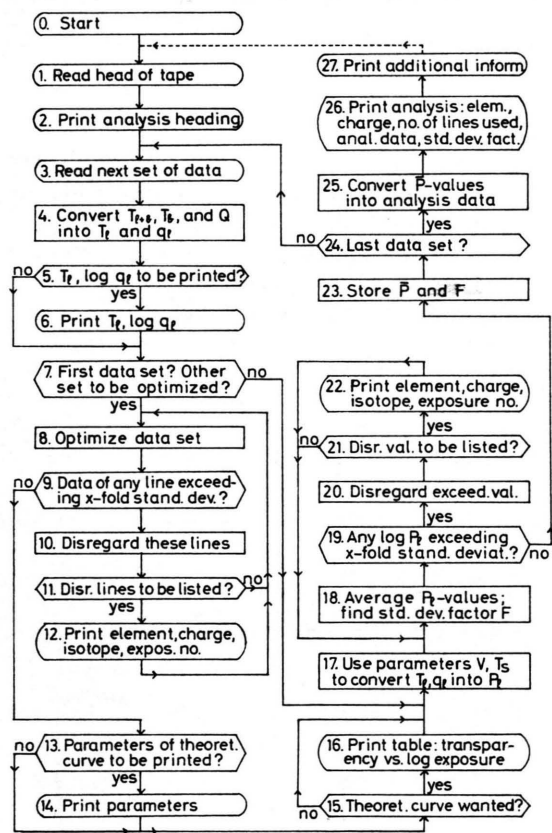


Fig. 3. Simplified flow chart of the program for photographic plate evaluation. The flexibility of performance of steps 3, 4, and 24 is shown in detail in Fig. 4.

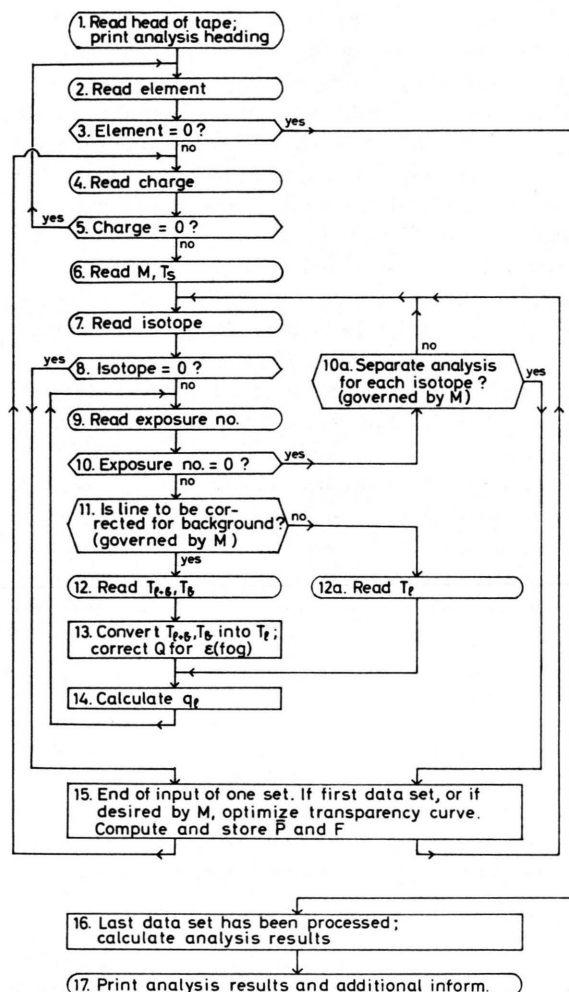


Fig. 4. Simplified flow chart of the photoplate evaluation program, showing the flexibility of data input. The input paper tape contains the information in the following sequence: element, charge, submodus number  $M$ , saturation transparency  $T_s$ , isotope, exposure number  $n$ , line transparency  $T_{1+b}$ , and background transparency  $T_b$ . Then another number triple ( $n$ ,  $T_{1+b}$ ,  $T_b$ ) [or the couple ( $n$ ,  $T_b$ ) if plate background is not to be corrected] appears until an end mark breaks the cycle. The end mark „0“ indicates a new isotope, two zeros („0; 0“) mark a new charge of the same element. Three zeros („0; 0; 0“) mark a new element, and four consecutive zeros („0; 0; 0; 0“) mark the end of the analysis. For example, at the end of analysis, the first zero after the last number triple ( $n$ ,  $T_{1+b}$ ,  $T_b$ ) is read in step 9, leading to step 7 via steps 10 and 10 a. In step 7 the next zero is read, leading to step 4 via step 15. In step 4 the third zero leads back to step 2, where the fourth zero indicates the end of the analysis. Then the program jumps from step 3 to step 16: it calculates, and then prints, the total analysis. It should be noted that step 15 of the flow chart contains steps 5 to 23 of Fig. 3. The submodus number  $M$  determines whether background correction is to be made, whether a separate analysis is wanted from each isotope, and whether a new set of data is to be optimized.

graphic sensitivity, the law of line area correction, and the units in which the analysis is to be printed out; finally, the data  $Q$  of the different exposures on the plate (or plates in case of modus 9). In steps 3 and 4, the information on the line on hand is read (element, charge, submodus, isotope). The program then reads the exposure numbers, line transparencies  $T_{1+b}$ , and background transparencies  $T_b$  (as will be shown in detail in Fig. 4), immediately converting these into  $(T_1, q_1)$ -values. Steps 5 to 24 are self-explanatory in view of the discussion of the previous chapters. In step 25, the program differentiates between the different modi. We recall that eq. (8) for  $\bar{P}$ , which is readily available from the computer storage, contains the concentration  $C$ , the absolute photographic sensitivity  $e_{\text{abs}}$ , and the relative sensitivity  $s$  of ion formation. Depending on the modus chosen, eq. (8) is solved for one of these three quantities; the remaining two unknown quantities have to be eliminated by forming the ratio

$$R = \frac{\bar{P}_{\text{anal}}}{\bar{P}_{\text{ref}}} = \frac{C_{\text{anal}} \cdot (e_{\text{abs}})_{\text{anal}} \cdot s_{\text{anal}}}{C_{\text{ref}} \cdot (e_{\text{abs}})_{\text{ref}} \cdot s_{\text{ref}}} \quad (15)$$

In modus 1, only applicable if the analysis is based on the evaluation of singly-charged ion species,  $e_{\text{abs}}$  is assumed to be constant over the entire plate, and  $s$  is assumed to be equal for all elements. The sought concentration  $C_{\text{anal}}$  of the analyzed element is then given by

$$C_{\text{anal}} = R \cdot C_{\text{ref}}, \quad (16)$$

where  $C_{\text{ref}}$  is the concentration of a reference element in the sample (e.g. main sample component  $\approx 100\%$ , or internal reference), known beforehand and contained in the data input.

In modus 2 which is not limited to singly-charged ion species, the known sensitivity factors  $s$  can be used to find

$$C_{\text{anal}} = R \cdot C_{\text{ref}} \cdot s_{\text{ref}} / s_{\text{anal}} \quad (17)$$

In modus 3 the known concentrations  $C_{\text{anal}}$  and  $C_{\text{ref}}$  can be employed to find

$$s_{\text{anal}} / s_{\text{ref}} = R \cdot C_{\text{ref}} / C_{\text{anal}} \quad (18)$$

In modus 4 we might want the ratio of the absolute photographic sensitivity from two regions of one plate, or from two plates:

$$(e_{\text{abs}})_1 / (e_{\text{abs}})_2 = R, \quad (19)$$

provided  $C_1 = C_2$  and  $s_1 = s_2$  which is true if, for example, the same sample was used in both cases.

Modus 5 and modus 6 for the determination of molecular ion abundance ratios, and for the determination of isotope abundance ratios, can be traced back to modus 1.

For precision analyses, the absolute photographic sensitivity  $e_{\text{abs}}$  cannot be assumed constant along the plate (we have observed fluctuations of  $e_{\text{abs}}$  of a factor 5 in the extreme within a few cm of a plate). Therefore, in case of modi 7 and 8, a reference spectrum is exposed on the same plate as the analytical spectrum such that related lines of the analytical sample and the reference sample are closely neighboured, as shown in Fig. 5. With this technique,  $e_{\text{abs}}$  surely remains constant. With modus 7 we obtain the isotope abundance ratio

$$\frac{h(\text{isotope 1})_{\text{anal}}}{h(\text{isotope 2})_{\text{anal}}} = R \cdot \frac{h(\text{isotope 1})_{\text{ref}}}{h(\text{isotope 2})_{\text{ref}}}, \quad (20)$$

with modus 8 we get the concentration as in eq. (16).

Modus 9 is a condensation of modi 2 and 3.

### Flexibility of Data Input

The number of evaluated lines varies strongly from plate to plate; therefore, a varying number of input data have to be accepted by the computer. This is achieved by the introduction of end marks which we decided to be zeros. Details of the data input are shown in the flow chart of Fig. 4.

### Computer-obtained Precision of Photoplate Evaluation

To demonstrate the precision which can be obtained by the algorithm described above, we have exposed a number of plates with mass spectra from

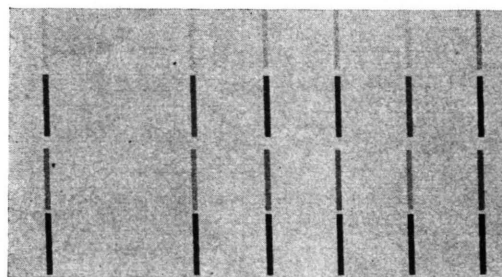


Fig. 5. Part of a mass spectrum of the reference samples SS 5 and SS 6, showing several exposures of the lines  $^{92}\text{Mo}^{2+}$  through  $^{98}\text{Mo}^{2+}$ . The exposures were alternated, i. e. every other exposure belongs to the same sample.



two stainless steel samples<sup>12</sup>. Fig. 5 shows a portion of one such spectrum, limited to the lines of  $\text{Mo}^{2+}$ . We have chosen the molybdenum lines to demonstrate the precision of evaluation because this element has a relatively large number of isotopes. In case of  $\text{Mo}^{2+}$  and  $\text{Mo}^{3+}$  we evaluated the lines of six isotopes each, for  $\text{Mo}^{4+}$  there were only four isotopes undisturbed. If the computer program is controlled such that a separate analysis is made for each isotope, we obtain 16 independent analyses of Mo from each plate. The evaluation of nine plates with a total of 144 analyses should therefore yield sufficient statistics. The spectra of  $\text{Mo}^{3+}$  and  $\text{Mo}^{4+}$  are not shown here but they are of comparable quality to that of  $\text{Mo}^{2+}$ . For evaluation, we have used a photometer slit area of  $60 \times 1000 \mu\text{m}^2$  for  $\text{Mo}^{2+}$ , and  $40 \times 1000 \mu\text{m}^2$  for  $\text{Mo}^{3+}$  and  $\text{Mo}^{4+}$ .

It is easy to estimate the precision of evaluation theoretically expected from a consideration of grain statistics<sup>9</sup>: if a number of lines, exposed identically to give a mean transparency of 50%, are measured accurately with a photometer, the photometer reading will vary from measurement to measurement due to the statistics of the Ag grains lying within the photometer slit area. Since the Ag grains of ILFORD Q 2 emulsions have a mean projection area of approximately  $1 \mu\text{m}^2$ , a line with 50% transparency will contribute about  $G = 3 \cdot 10^4$  Ag grains to a slit of  $60 \times 1000 \mu\text{m}^2$  area. The standard deviation  $\sigma(G)$  of the number of grains  $\bar{G}$  is equal to  $\sqrt{\bar{G}} = \sqrt{3 \cdot 10^4} = 170$ , hence the relative standard deviation is

$$\sigma(G)/\bar{G} = \sigma(T)/\bar{T} = 0.0058.$$

From the transparency curve (see Fig. 1 or 2) we find a factor of about 2.5 for the conversion of transparency fluctuations at 50%  $T_1$  into  $P_1$ - or  $C$ -fluctuations. This factor yields an expected precision of about 0.015 relative standard deviation, in agreement with the value reported earlier<sup>9</sup>. In case of a slit area of  $40 \times 1000 \mu\text{m}^2$ , we expect a precision of about 0.018 relative standard deviation. There are always several lines used for one analysis; hence the precision of the results will improve with  $1/\sqrt{n}$ , where  $n$  = number of lines used. On the other hand there is, in general, not more than one line with a transparency of 50%. The remaining lines usually fall on portions of the transparency curve

with smaller slope, resulting in a decrease of precision. Therefore, these lines add but little to the overall precision. The net precision obtainable in practice will be somewhat better than the precision obtained for one line only, provided this line exhibits the optimum transparency of 50%.

We have evaluated our nine plates with modulus 8 of the computer program (calculation of concentrations in sample SS 5 by comparison with sample SS 6 as reference). In general operation, the program combines all isotopes of one element with given charge to yield the analysis of that element. In the present case, we have, for demonstration, controlled the program by a change of submodus to give a separate analysis for each isotope. In table 1, the mean values of the analyses obtained

Plate no.	mean concentration (% by weight) of six analyses $^{92}\text{Mo}^{2+} - ^{98}\text{Mo}^{2+}$	relative standard deviation
1	1.388	0.013
2	1.358	0.012
3	1.358	0.010
4	1.341	0.011
5	1.378	0.024
6	1.562	0.008
7	1.531	0.018
8	1.434	0.008
9	1.345	0.012

Table 1. The mean concentration varies from plate to plate due to sample inhomogeneities in the SS 6 reference.

from the six isotopes of  $\text{Mo}^{2+}$  on each plate are shown together with their relative standard deviations. We notice that the concentration fluctuations from plate to plate are larger than what would be allowed by the relative standard deviations of the six analyses from one plate. This fact can be interpreted unambiguously by poor homogeneity of Mo in the reference sample SS 6. Similar tables may be set up for  $\text{Mo}^{3+}$  and  $\text{Mo}^{4+}$ . The relative standard deviations shown in table 1 are statistically insignificant because they were obtained from six values only. In order to arrive at a statistically significant number, all 54 available analyses should be correlated. If the relative standard deviation is calculated in the usual manner, i.e. if the deviations of all 54 analyses from the mean are used, the resulting relative standard deviation contains both the fluctuations due to photoplate grain statistics and the fluctuations due to sample inhomogeneities. To eliminate the influence of the latter, a statistical

<sup>12</sup> Samples SS 5 and SS 6, Bureau of Analysed Samples, Ltd., England.

treatment by group formation is indicated. This is done by

$$s_{\text{rel}} = \sqrt{\frac{\sum e_i^2}{n-g}} / \bar{c}, \quad (21)$$

where

$$e_i = c_i - \bar{c}_g,$$

$n$  = total number of individual values  $c_i$ ,

$g$  = number of groups and

$\bar{c}, \bar{c}_g$  = total mean and group mean of individual values.

The relative standard deviations found by defining one such group to contain the six ( $\text{Mo}^{2+}$ ,  $\text{Mo}^{3+}$ ) and four ( $\text{Mo}^{4+}$ ) analyses from one plate are shown in table 2. For  $\text{Mo}^{2+}$  and  $\text{Mo}^{3+}$  the relative standard

	$\text{Mo}^{2+}$	$\text{Mo}^{3+}$	$\text{Mo}^{4+}$
rel. stand. dev. according to eq. (21)	0.014	0.016	0.045
total number of analyses	54	54	36
photometer slit area	0.06 mm <sup>2</sup>	0.04 mm <sup>2</sup>	0.04 mm <sup>2</sup>
avg. number of lines evaluated per analysis for SS 5 and SS 6, respectively	3-5	3-4	1-3

Table 2.

deviations found, 0.014 and 0.016, are in close agreement with the values theoretically predicted. The larger deviation of the  $\text{Mo}^{4+}$  analyses can be explained by the fact that frequently only one faint line could be evaluated for analysis. It should be pointed out that the given relative standard devia-

tions contain the fluctuations of *both* the analytical sample (SS 5) and the reference sample (SS 6).

To indicate the capability of the program for analysis work and to somewhat rectify the general opinion on the much-abused photoplate, we have determined the abundances of the molybdenum isotopes with modus 7 of the computer program. Table 3 shows the various abundance ratios for  $\text{Mo}^{2+}$ ,  $\text{Mo}^{3+}$ , and  $\text{Mo}^{4+}$ , as well as the weighted mean abundance values as obtained from 10 plates, normalized to  $^{98}\text{Mo}=100\%$ , and compared with the tabulated values<sup>13</sup> which were assumed to hold for the reference sample SS 6.

### Technical Details

The program is written in ALGOL and takes about 7000 words storage space. Another 4000 storage words are needed during the calculation. The names of the elements, the isotope abundances, and the atomic weights are listed in the program. The program has been especially written for use with a SIEMENS 2002 computer. It can easily be modified for use with other computers accepting ALGOL.

We are indebted to Prof. Dr. H. HINTENBERGER for his interest in the present work. We are further grateful to the Institute of Applied Mathematics, University of Mainz, for the generosity with which ample computer time was granted; in particular we should like to express our sincere thanks to TH. HANSEN from that Institute for the many fruitful discussions we had.

	$^{100}\text{Mo}$	$^{98}\text{Mo}$	$^{97}\text{Mo}$	$^{96}\text{Mo}$	$^{95}\text{Mo}$	$^{94}\text{Mo}$	$^{92}\text{Mo}$
$\text{Mo}^{2+}$	—	100	40.05	69.49	65.96	38.58	66.67
$\text{Mo}^{3+}$	40.49	100	40.61	—	65.72	37.89	66.56
$\text{Mo}^{4+}$	—	100	39.95	—	67.53	39.52	—
weighted mean of 10 plates	40.49	100	40.15	69.49	66.13	38.20	66.62
absolute stand. dev.	$\pm 0.24$		$\pm 0.22$	$\pm 0.41$	$\pm 0.32$	$\pm 0.17$	$\pm 0.30$
tabulated values	40.496	100	39.781	69.512	66.105	38.015	66.610

Table 3. Isotope abundance analysis with modus 7 of the computer program: the spectra of sample SS 5 were compared with those of sample SS 6 on the same plate. The tabulated abundance ratios<sup>13</sup> were assumed to hold true for the molybdenum isotopes in sample SS 6. The mean values given are the weighted averages from the separate evaluation of  $\text{Mo}^{2+}$ ,  $\text{Mo}^{3+}$ , and  $\text{Mo}^{4+}$ . The weights  $p=1/\sigma^2$  were obtained, for each charge, from the relative standard deviations  $\sigma$  of the individual ratios  $m\text{Mo}/^{98}\text{Mo}$  from ten plates. The  $\pm$ -figures given represent the absolute standard deviations of the weighted mean values.

<sup>13</sup> Chart of the Nuclides, 2nd ed., Fed. Minister of Nuclear Energy, Bad Godesberg, Germany, literature revised up to July 1961.